Bowed-string multiphonics analyzed by use of impulse response and the Poisson summation formula

Knut Guettler[a]

Norwegian State Academy of Music, Eilins vei 20, 1358 Jar, Norway

Håkon Thelin

Norwegian State Academy of Music, P. O. Box 5190 Majorstua, 0302 Oslo, Norway

By carefully positioning the bow and a lightly touching finger on the string, the string spectrum can be conditioned to provide narrow bands of pronounced energy. This leaves the impression of multiple complex tones with the normal (Helmholtz) fundamental as the lowest pitch. The phenomenon is seen to be caused by two additional signal loops, one on each side of the finger, which through the repeating slip pattern get phase locked to the full loop of the fundamental. Within the nominal period, however, the slip pulses will not be uniform like they are during the production of a normal "harmonic" or "flageolet" but may vary considerably in shape, size, and timing. For each string, there is a large number of bow/finger combinations that bear the potential of producing such tones. There are also two classes, depending on whether the bow or the finger is situated closest to the bridge. Touching the string with the finger closest to the bridge will somewhat emphasize the (Helmholtz) fundamental. The technique is applicable to double bass and cello, while less practical on shorter-stringed instruments. Analyses based on impulse responses and the Poisson summation formula provide an explanation to the underlying system properties.
© 2012 Acoustical Society of America. [DOI: 10.1121/1.3651251]

I. INTRODUCTION

Multiphonics in wind instruments has been around for a while. Nowadays you often hear saxophone players utilizing the technique in jazz and contemporary music. In brass instruments, the effect dates back even longer and even is found in music from the classical period (e.g., in the horn concerto from 1806 by Carl Maria von Weber). Here the musician sings along with the lip-controlled pitch and thus creates a quite audible series of difference tones. Woodwind players mostly use quite special fingering in combination with very precise embouchure.

In string instruments, multiphonics is mainly a filtering technique where the potential energy of certain partials of an (in most cases) open-string fundamental is restrained by a left-hand finger pad lightly touching the string. This favors the conditions for some of the remaining partials, separately or in narrow clusters. See Fig. 1 for a typical sound spectrum of a double bass played with the lightly touching finger four-and-a-half semitones up the string, and the bow placed at the seventh-harmonic node. (Here, α denotes the finger position relative to the string length, λ denotes relative string-length decrement per semitone ≈ 0.9439, the power of which thus denoting the number of semitones, while β denotes the relative bow position on the string with respect to the bridge). In Fig. 1 the corresponding decimal values for α and β are approximately 0.77 and 0.14, respectively.

Although performed by Italian double bassist Fernando Grillo[1] during the first part of the 1970s, with similar effects already being utilized by Hungarian György Ligeti in his work "Apparitions" from 1958 to 1959, the first comprehensive description of multiphonics is dated to 1995 when French bassist Jean-Pierre Robert published his bilingual book "*Les Modes de jeu de la Contrabasse—Un Dictionnaire de Son/Modes of Playing the Double Bass—A Dictionary of Sound*" in collaboration with IRCAM.[2] This research, which started in 1985, also made a noticeable impact on composers working in Paris and IRCAM at the same time. A similar description on the production of multiphonic sounds was later found in the article "A personal pedagogy" by Mark Dresser.[3] Dresser has been further exploring multiphonics, without being much influenced by the European achievements, and his discoveries were presented in several articles published in The Strad.[4]

A comprehensive and detailed study on multiphonics on the double bass was later presented by Michael Liebman in his article "Multiphonics: new sounds for double bass," which unfortunately has remained unpublished. His study on new sonic opportunities of string instruments began in 1997 and manifested itself quickly in the composition *Movement of Repose* (1998) for cello and the article "Multiphonics Neue Moglichkeiten im Cellospiel (Multiphonics, new possibilities in cello playing)."[5] In the material from Robert, Liebman, and Dresser, we find extensive information about the technical production and timbre variations of multiphonics sounds, together with chord schemes (spectral analysis) that illustrate the most known multiphonics. However, the acoustical implications in terms of string waveforms, etc. were never touched upon by these authors.

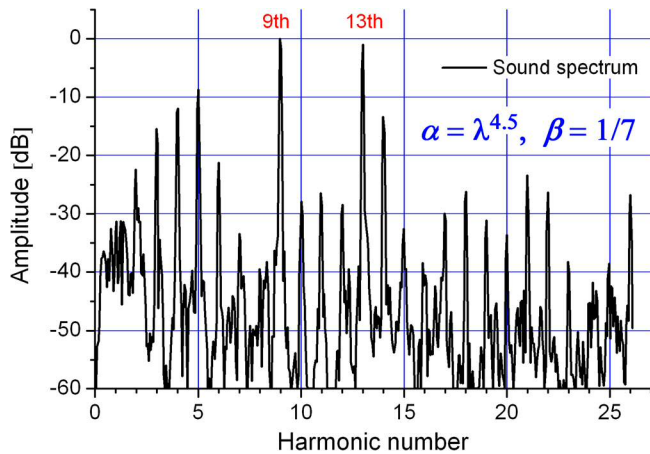[a]Author to whom correspondence should be addressed. Electronic address: knut.guettler@tele2.no

FIG. 1. (Color online) Sound spectrum of a multiphonics played on the double-bass E-string with the lightly touching finger at $\alpha = \lambda^{4.5} \approx 0.77$ (relative string length), and the bow at $\beta = 1/7 \approx 0.14$ (relative string length). Harmonics 9 and 13 are clearly emphasized in the spectrum while harmonics in between are restrained.

II. MEASURING METHOD

To clarify how the string moves, a hybrid technique was utilized in our experiments: After a traditional recording of the string movement under the bow, i.e., with a strong magnet placed directly under the string and a registration of the difference in voltage potential at the two string ends, the resulting (velocity) signal could be fed as the bow-velocity input to a bowed-string simulation program.[6] By combining this signal with a bow force that ensures a static-friction grip at all times—and some suitable string-end and touching-finger

reflections, the characteristic movements of the entire string could be visualized and analyzed.[10] (Conveniently, the string cannot "see" the difference between static and dynamic friction, only the resulting frictional force, which also can be derived from the simulation itself provided the string impedances and the other parameters are correctly defined.) This proved to be a very convenient way of getting an overview over otherwise quite complex phenomena and enabled us to produce a slow-motion animation of every multiphonics member, as well as estimating the force acting on the bridge.

With a fixed bow position on the string, a series of unique sound spectra can be obtained by moving the lightly touching finger along the string length. We recorded a selection from two such series on an open double-bass E-string: one with the bow placed at the point $\beta = 1/7$ of the string length from the bridge and another one where β was 1/13. These are shown in Figs. 2 and 3, respectively. Spectral analyses were done both from the string signal itself and from an audio signal picked up with a normal microphone in the near field of the instrument. In the plots, α indicates the position of the lightly touching finger (measured from bridge), relative to the vibrating string length, while λ indicates the relative string-length decrement per semitone, that is: $\lambda = \mathrm{Exp}[-\ln(2)/12] \approx 0.9439$. Thus the exponent of λ gives the number of semitones above the pitch of the open string, while the decimal 0.5 denotes a quartertone.

Normally, finger positions with the potential of producing "normal harmonics" (flageolet tones) are avoided. This implies staying away from nodes of, say, the six lowest harmonics. However, with a careful choice of bow speed and
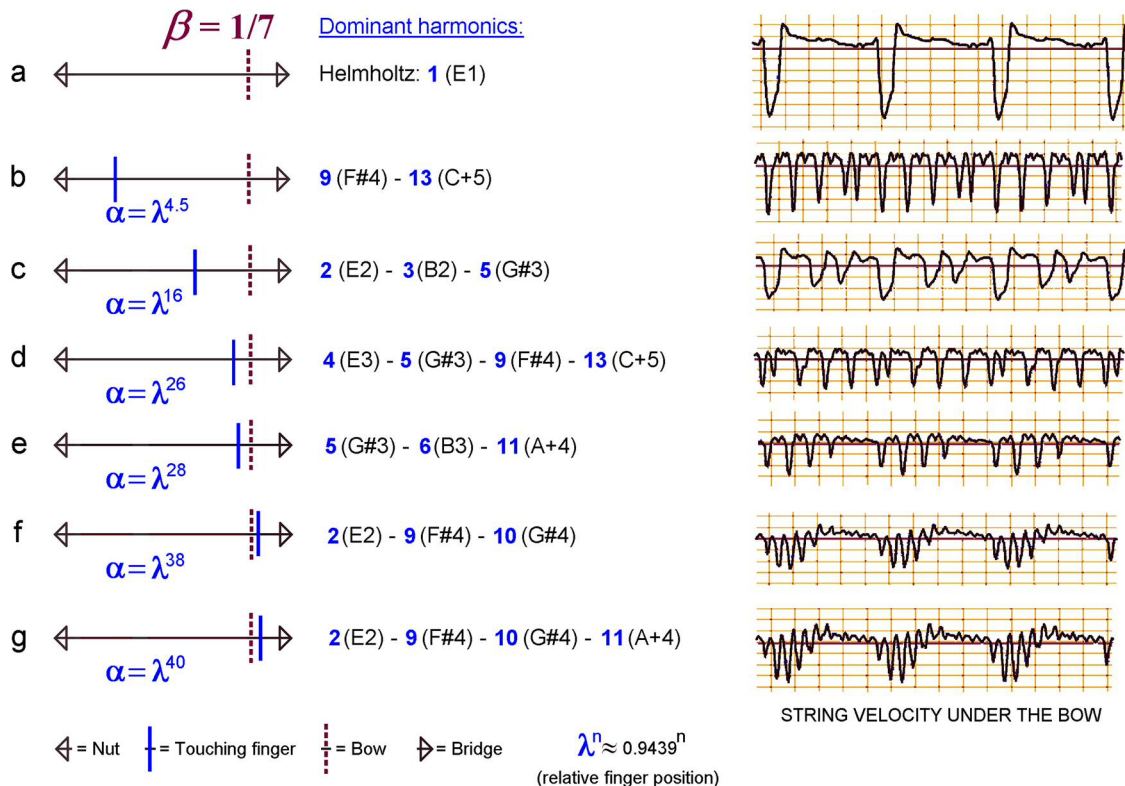

FIG. 2. (Color online) Examples of practical multiphonics (b–g) based on bow position, $\beta = 1/7 \approx 0.14$, compared to Helmholtz motion (a). Left column shows finger- and bow positions on the string as seen by the player. Middle column indicates dominant harmonics (bold harmonic numbers and musical pitches) as measured with microphone in the near field. Right column shows string wave forms under the bow.
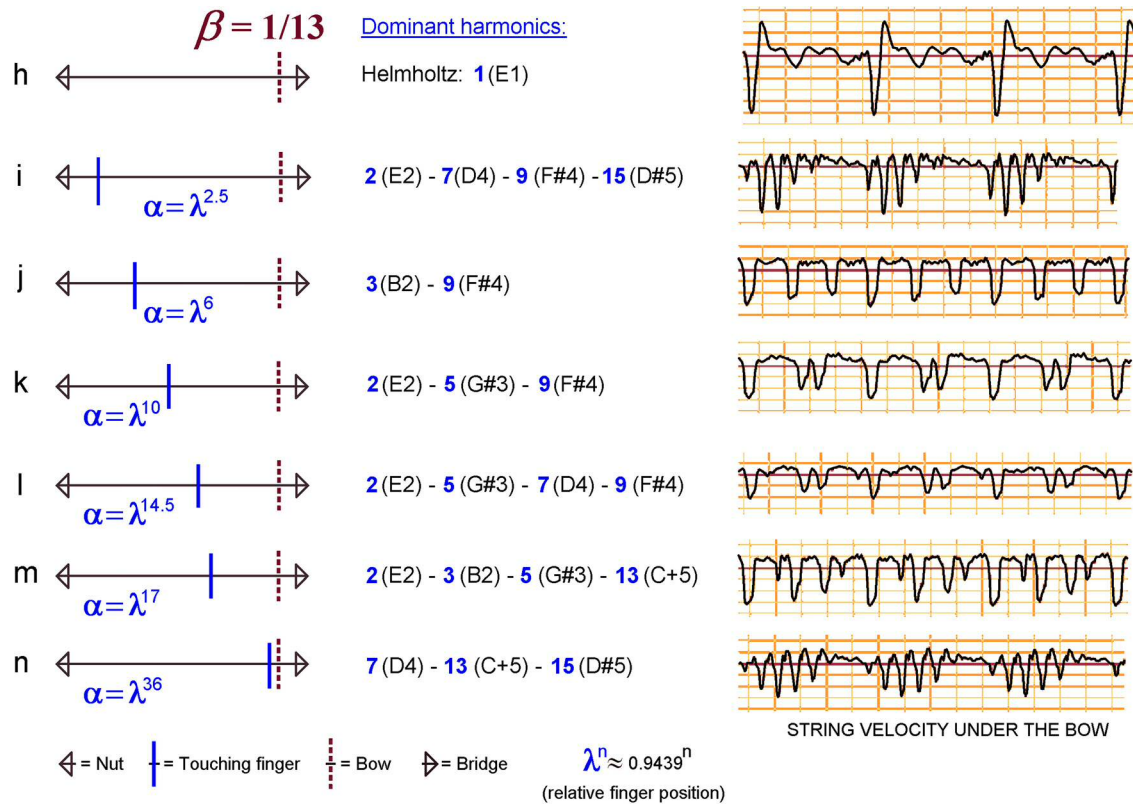
β = 1/13   Dominant harmonics:

h   Helmholtz: **1** (E1)

i   **2** (E2) - **7** (D4) - **9** (F#4) - **15** (D#5)
$\alpha = \lambda^{2.5}$

j   **3** (B2) - **9** (F#4)
$\alpha = \lambda^{6}$

k   **2** (E2) - **5** (G#3) - **9** (F#4)
$\alpha = \lambda^{10}$

l   **2** (E2) - **5** (G#3) - **7** (D4) - **9** (F#4)
$\alpha = \lambda^{14.5}$

m   **2** (E2) - **3** (B2) - **5** (G#3) - **13** (C+5)
$\alpha = \lambda^{17}$

n   **7** (D4) - **13** (C+5) - **15** (D#5)
$\alpha = \lambda^{36}$

◁ = Nut | = Touching finger   ┊ = Bow   ▷ = Bridge $\lambda^n \approx 0.9439^n$
(relative finger position)

STRING VELOCITY UNDER THE BOW

FIG. 3. (Color online) Examples of practical multiphonics (i–n) based on bow position, $\beta = 1/13 \approx 0.077$, compared to Helmholtz motion (h).

force (lower and greater, respectively), flageolet tones can be avoided in any case. In Figs. 2 and 3, the left column indicates finger- and bow positions as seen by the player. The middle column indicates the resulting dominant harmonics both by number and pitch, while the right column shows string waveforms under the bow. Notice that in Fig. 2, examples f and g (with $\alpha = \lambda^{38}$ and λ^{40}, respectively) are of class one with the finger touching the string between the bow and the bridge, while the remaining ones are of class two, i.e., with the finger on the nut side of the bow. Although members of class one multiphonics respond better and are easier to play, members of class two are more often employed as these offer a greater variety of sonorities.

As is seen in Figs. 2 and 3, right column, where the string's velocity for a little more than three nominal periods are plotted, each multiphonics has more than one slip (pulse with significant negative velocity) per period. These vary in both width and velocity. For the two last examples of Fig. 2, the waveform shows a long sticking interval followed by a series of short slips. This is typical for the class one members. During the stick interval, the string behaves pretty much like under normal Helmholtz conditions, although several "corners" can be seen traveling in succession. Figure 4 shows examples of string shapes (upper panel) and the respective force on the bridge (lower panel) as calculated with the simulation program when using the measured bowing-point string velocity as input.[10] Unlike in *ponticello* playing, where the number of slips per nominal period usually determines which harmonic number dominates (with spectral slopes on both sides), the spectral profiles of the multiphonic members appear far more complex.

III. IMPULSE-RESPONSE ANALYSIS

A. Signal bookkeeping

1. Class one

To understand the filtering mechanism, it is useful to look at the impulse response with the lightly-touching finger on the string. By use of a simulation program, the important parameters, particularly bow and finger positions, can be defined and utilized for impulse-response experiments. In this connection, the finger can be regarded as purely resistive with convenient reflection and transfer coefficients both equal to 0.5, while disregarding further losses. With absolute (amplitude) reflection coefficient $\gamma = 0.5$, half the energy is dissipated in the finger: the relative reflected energy, $R_E = \gamma^2$; the relative transmitted energy, $T_E = (1 - \gamma)^2$; the relative dissipated energy, $D_E = 1 - R_E - T_E$. Our simulations suggest that the value of γ is not of significant importance for the spectral profile within the range $0.2 < \gamma < 0.8$. Neither is the profile very sensitive to the losses at nut and bridge provided these are reasonably small.

Figure 5 (example of class one—bow on the nut side of the finger) shows the force on the bridge during the first 1.3 nominal periods after a unit impulse is given at the bowing point, β, at the time $t = 0$. The letters E, B, F, and N stand for excitation point (i.e., bowing point), bridge, finger, and nut, respectively, and indicate the paths of the impulses arriving at the bridge. As is seen, there are two trains of fading impulses, one negative and one positive, both with intervals of Tα (where T is the nominal period of the unfingered string), but
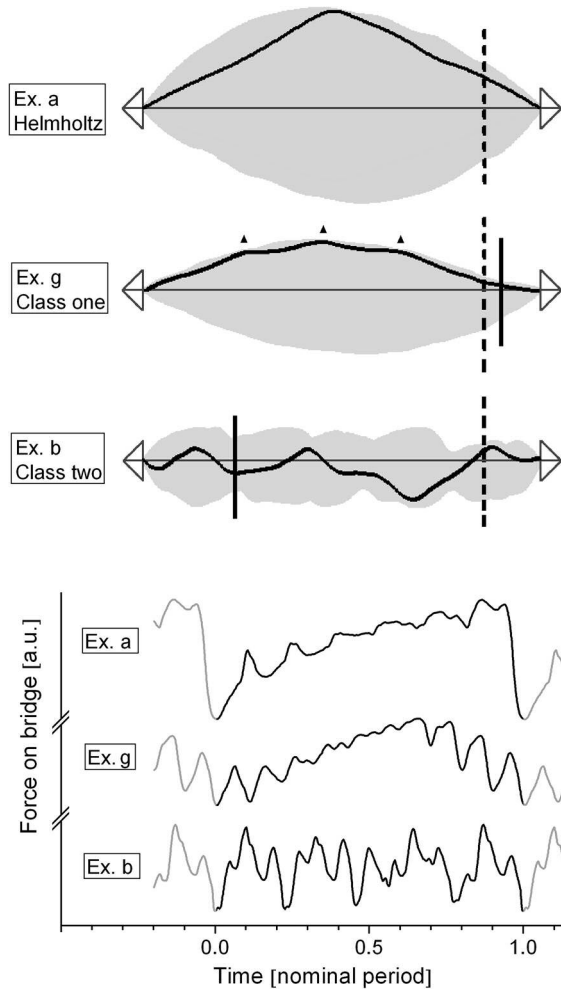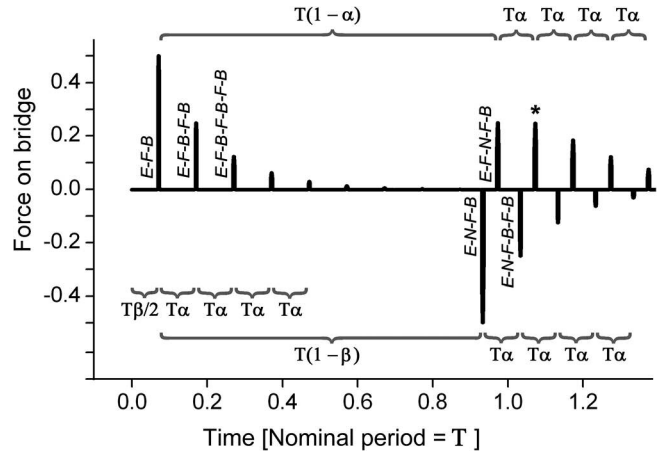
FIG. 5. The first part of a simulated impulse response (force on the bridge) for multiphonics of class one. The letters E, B, F, and N stand for excitation point (i.e., bowing point), bridge, finger, and nut, respectively, and are indicating the paths of the impulses arriving at the bridge. The impulse marked with an asterisk is a result of concurrent impulses arriving from two different paths.

FIG. 4. Characteristic string shapes (upper panel) and force signals on the bridge (lower panel). Reconstructions are based on actual string-velocity signals recorded under the bow. The letters a, b, and g refer to the examples shown in Fig. 2. Members of class one (e.g., example g) resemble to some degree the Helmholtz motion but differ from this mode in that they comprise several rotating corners (some of which are marked with spikes in the upper panel). These corners cause a series of *non-uniformed* slips within each nominal period.

the negative series shifted $T(1-\beta)$ with respect to the positive one, as it has taken one turn to the nut before entering the bridge area. Because the impulses fade out with a factor γ for each repeated reflection at the finger, we can roughly describe it as a series of Dirac deltas on the bridge side (ignoring the very first $T\beta/2$ delay and minor losses at the bridge and nut):

$$\sum_{k=1}^{\infty} \gamma^k \{\delta[t - T k\alpha] - \delta[t - T(k\alpha + 1 - \beta)]\},\qquad (1a)$$

where δ is the Dirac delta and γ is the absolute reflection coefficient.

The delay term $T(1-\beta)$ describes the initial impulse traveling directly to the nut before returning to the bridge area. Moreover, a fading signal will be looping between the nut and the finger:

$$\sum_{k=1}^{\infty} \gamma^k \{\delta[t - T k(1-\alpha)] - \delta[t - T\{k(1-\alpha) + 1 - \beta\}]\}.$$

$$(1b)$$

But, of course, these will only have consequences after entering the bridge side. The reason we make this approximation is that it tells us something about the profile of the resulting impulse-response spectrum. Taking the Fourier transforms of Eqs. (1a) and (1b), we get:

$$\sum_{k=1}^{\infty} \gamma^k \{Exp[j T k\alpha\omega] - Exp[j T(k\alpha + 1 - \beta)\omega]\},\qquad (2a)$$

where $j = \sqrt{-1}$ and ω is the angular frequency: $2\pi f$, and

$$\sum_{k=1}^{\infty} \gamma^k \{Exp[j T k(1-\alpha)\omega] - Exp[j T(k(1-\alpha) + 1 - \beta)\omega]\},$$

$$(2b)$$

respectively. We see that due to pair-wise symmetry, Eqs. (2a) and (2b) will both go to zero whenever $\omega = n2\pi/T(1-\beta)$, $(n = 1, 2, 3,...)$, i.e., for harmonic frequencies of the delay period $T(1-\beta)$. Notice, however, that the expressions in the preceding text are not the only ones relevant for describing existing loops. For instance, there is the loop of the full string length, which has a decrement factor of $(1-\gamma)^2$ per period, T. The contribution of this loop is mainly seen in slight shifts toward harmonicity for resonances already discussed. Unarguably, Eqs. (1a) and (1b) constitute the most significant factors in terms of understanding how the spectrum is shaped.

2. Class two

In a similar way, we can construct some approximate expressions for class-two multiphonics (bow on the bridge side), although to obtain pair-wise symmetry, we temporarily have to ignore the very first impulse of Fig. 6, arriving at the bridge at $t = T\beta/2$ and counting from there.

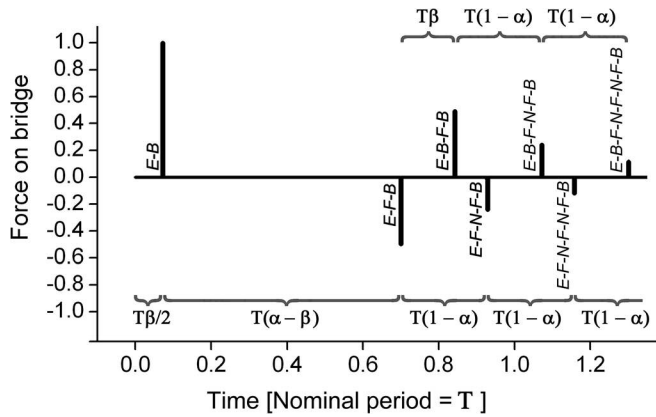For the signal looping between the bridge and the finger we can write:

FIG. 6. The first part *a* of simulated impulse response (force on the bridge) for multiphonics of class two.

$$\sum_{k=1}^{\infty} \gamma^k \{\delta[t - T(k\,\alpha - \beta)] - \delta[t - Tk\,\alpha]\}, \tag{3a}$$

and for the signal on the nut side of the finger:

$$\sum_{k=1}^{\infty} \gamma^k \{\delta[t - T\{k(1-\alpha) - \beta\}] - \delta[t - T k(1-\alpha)]\}. \tag{3b}$$

The elements of the corresponding Fourier transforms read:

$$\sum_{k=1}^{\infty} \gamma^k \{Exp[j\,T(k\,\alpha - \beta)\omega] - Exp[j\,T k\,\alpha\,\omega]\}, \tag{4a}$$

and

$$\sum_{k=1}^{\infty} \gamma^k \{Exp[j\,Tk(1-\alpha)\omega] - Exp[j\,T\{k(1-\alpha) - \beta\}\omega]\}. \tag{4b}$$

These last two expressions both equal zero for frequencies, $\omega = n2\pi/(T\beta)$, $(n = 1, 2, 3, \ldots)$, but after adding the transform of the missing first impulse (i.e., unity for all ω) the effect is reduced and the cancellation only partial (a minimum magnitude value will appear).

Notice, the filtering effects described in the preceding text for multiphonics of classes one and two are not simply modifying an established waveform such as the Helmholtz mode[11] or any higher type of Raman vibrational modes.[12] (Evidence of this can be found through deconvolving[13] the multiphonic string signal under the bow with the impulse-response signal at the same place, followed by a convolution with the impulse signal of the free, unobstructed, string, or, alternatively, through convolving a Helmholtz signal with a class-one impulse-response signal followed by a deconvolution with the free-string impulse response.) The filtering rather defines the waves' environment on the string, i.e., the conditions for different frequencies to develop and survive there, while the resulting mode appears as a matter of the consequent *nonlinear* stick-slip action. However, closest to the Helmholtz mode is multiphonics of class one, where a number of successive corners are rotating on the string with

the same orientation as the single corner during Helmholtz motion. No such rotation is apparent in class two. One should also remember that in class two, where no filtering object is positioned between the bow and the bridge, the resulting force spectrum at the bridge is uniquely defined by the string's (slip-stick) wave pattern under the bow, with no further concern to the finger's filtering on the nut side (this inverse-multi-lobe transfer function is described by Schoonderwaldt[14] and others).

3. Simulated spectra

Figures 7 and 8 show simulated impulse responses of classes one and two, respectively: The rectangular signal window was exactly 20 nominal periods long and so was the DTFT. No further windowing was utilized. Simulation parameters were: $\gamma = 0.5$; absolute reflection functions at bridge and nut: each 0.99 (resistive); no torsion or other losses; $\beta = 1/7 = 0.14$. The thick gray line indicates the continuous spectrum of the response. Magnitude minima and maxima of the continuous spectrum will only have consequences for the discrete harmonic spectrum as long as they coincide. Notice that in Fig. 7, we have notches in the continuous spectrum exactly where predicted from Eqs. (2a) and (2b), that is, relative frequencies $n/(1-\beta) = n/0.86$, which coincide with the harmonic numbers 7, 14, 21, etc., for $n = 6, 12, 18$. Notice also that the most prominent harmonics of Fig. 7 are the 9th, 10th, and 11th, just as measured from example g of Fig. 2. The major peak seen at harmonic 10 is controlled by the loop $T\alpha$ of Eq. (2a), which gives: $n/\alpha = n/0.1 = 10, 20, 30,\ldots$ for $n = 1, 2, 3$, etc.

In Fig. 8 (example of class two), the picture might appear less clear at first, although very sharp peaks in the continuous spectrum can be seen at harmonic frequencies 4, 8, 12, etc. These are related to the delay periods $T\alpha$ and $T(1 - \alpha)$ of Eqs. (3a) and (3b), respectively. In Eqs. (4a) and (4b), magnitude maxima are found for frequencies $m/(T\alpha)$, $(m = 1, 2, 3,\ldots)$
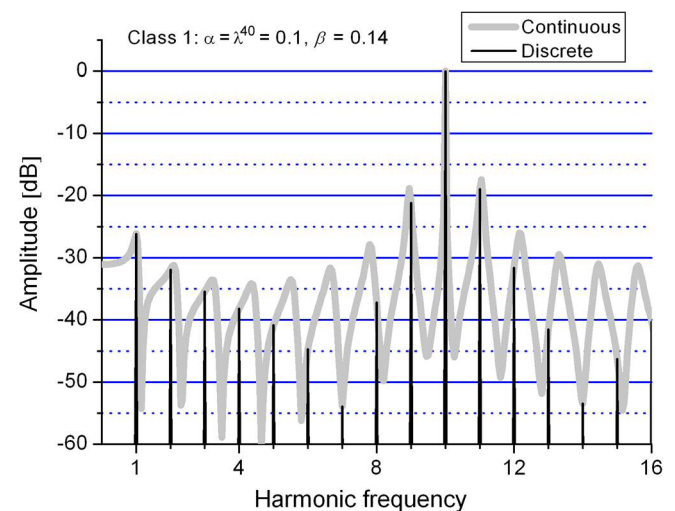

FIG. 7. (Color online) Spectra resulting from a class-one simulation ($\alpha = \lambda^{40} = 0.1$, $\beta = 1/7 = 0.14$). Gray thick line, continuous spectrum resulting from a normal impulse response; thin black lines, discrete spectrum resulting from impulses periodically repeated with intervals T, as predicted by the Poisson summation formula.
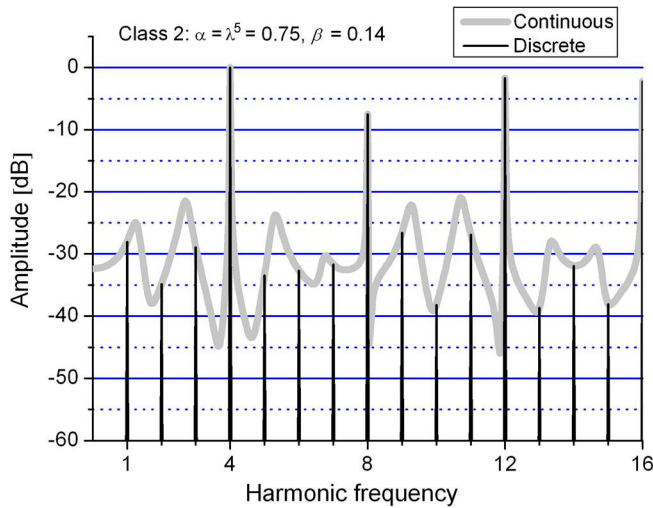
FIG. 8. (Color online) Spectra resulting from a class-two simulation ($\alpha = \lambda^5 = 0.75$, $\beta = 1/7 = 0.14$). Thick gray line, continuous spectrum resulting from a normal impulse response; thin black lines, discrete spectrum resulting from impulses periodically repeated with intervals T, as predicted by the PSF.
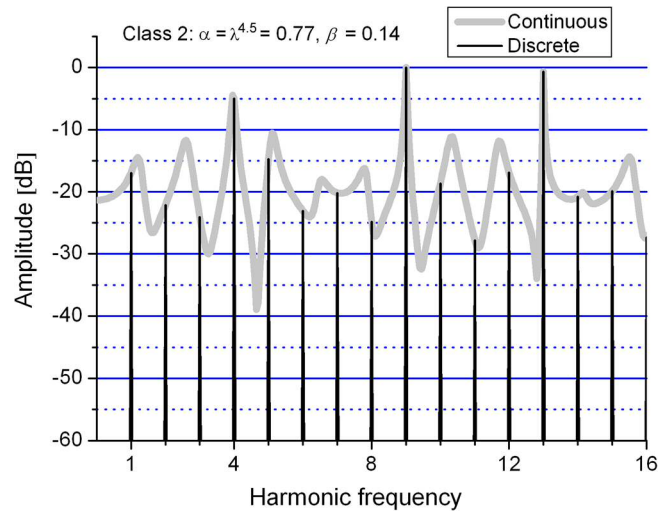

FIG. 9. (Color online) Spectra resulting from a class-two simulation ($\alpha = \lambda^{4.5} = 0.77$, $\beta = 1/7 = 0.14$). Thick gray line, continuous spectrum resulting from a normal impulse response; thin black lines, discrete spectrum as predicted by the PSF.

and for $n/[T(1-\alpha)]$, ($n = 1, 2, 3,…$), respectively. Where these two coincide, or nearly do so, the continuous spectrum will show major maxima, which again will have impact on the discrete spectrum if coinciding with the harmonic frequencies.

In the present case, $\alpha = \lambda^5 = 0.75$, so we get maxima for relative frequencies $m/0.75 = 1.33$, 2.67, 4.0, etc., and for $n/0.25 = 4, 8, 12$, etc., with major maxima at these harmonic numbers as seen in Fig. 8. Even though α indicates the position of a normal fourth harmonic (flageolet), the spectrum shown is indeed not of such a tone: The present spectrum is what you get if you draw the bow with fairly low speed and high force, adequate for multiphonics.

In our very first example of multiphonics (i.e., Fig. 1 and example b of Fig. 2), the parameter α was $\lambda^{4.5} = 0.77$. Accordingly, the expression $m/\alpha = 9.09$ and 12.99 for $m = 7$ and 10, while the expression $n/(1-\alpha) = 8.70$ and 13.04 for $n = 2$ and 3, respectively. These pairs of peaks fall close enough for the harmonics 9 and 13 to stand out exactly as was demonstrated at the outset. The simulated impulse response of this finger-bow combination and its belonging discrete harmonic spectrum are shown in Fig. 9. Notice that a quarter-tone adjustment (from semitone 5 to 4.5) of the lightly touching finger is all that was required for this spectral change to materialize.

B. The Poisson summation formula

In Figs. 7–9, we have actually anticipated the Poisson summation formula (PSF) by drawing in discrete lines for every harmonically related frequency up to the amplitude value of the continuous spectrum. While the continuous spectrum shows us the response of a single impulse at the time $t = 0$, we actually want to find the spectrum when periodic impulses are given at times $t = k \cdot T$, ($k = 0, 1, 2,…, \infty$). However, as the PSF will show, the resulting discrete spectrum can conveniently be estimated directly from the single-shot

impulse response when reading the Fourier-transform values for frequencies $f = n/T$, ($n = 1, 2, 3,…$) only, while ignoring the rest of the continuous spectrum. The PSF reads:

$$\sum_{k=\infty}^{\infty} f(x + 2\pi k) = \frac{1}{2\pi} \sum_{n=-\infty}^{\infty} \hat{F}(n)e^{inx}. \tag{5}$$

From this formula it can be deduced that given an impulse response with the continuous Fourier transform

$$\tilde{F}(\omega) := \int_{-\infty}^{\infty} f(t)e^{-i\omega t}dt, \tag{6}$$

the response of a *series* of identical impulses repeating with intervals of T will, provided convergence, add up to a Fourier transform with the discrete components

$$\tilde{F}(n) = \tilde{F}(\omega_\circ n), \quad (n = -\infty, .., -1, 0, 1, .., \infty), \tag{7}$$

where $\omega_0 = 2\pi/T$.

C. Relevance to airborne sound

The analyses in the preceding text are all based on the string's impulse signal and the resulting force on the bridge. In addition to the filtering in the string caused by the bow and the finger, the resonances and radiation of the instrument body are of course major factors in determining the final spectral outcome. With multiphonics produced on the lowest string, the lowest few harmonics will be poorly radiated by the instrument body, giving more emphasis on signal peaks above, provided they don't fall between body resonances. Likewise, due to the higher bending stiffness of lower strings, the range of harmonics that could potentially dominate will be limited also in the high end. The useful range of invocable harmonics seems to roll off around the twentieth. For that reason, strings without too great high-frequency damping are preferred. Another, more perceptual factor is that harmonics with numbers

2^n ($n = 1, 2, 3,...$) and $3 \cdot 2^m$ ($m = 0, 1, 2,...$) hardly will be noticed even when emphasized in the spectrum due to their quality of consonance (octaves and fifths) with respect to the fundamental pitch. Figure 4 displayed just that kind of situation. When regarding the middle columns of Figs. 2 and 3, it is striking that odd-numbered, dissonant harmonics dominate in this selection of musically desirable multiphonic members. Like in ordinary bowing, the spectral profile can be fine-tuned by the bow force but not on a detailed level.

IV. SUMMING UP

Through impulse-response analyses we have shown two classes of multiphonics. In both classes, we have seen impulse trains arrive at the bridge in pairs with opposite signs and with a delay between, but of (nearly) equal amplitudes so that they will cancel each other in certain parts of the spectrum. The delay is controlled by the position of the bow.

For class one, where $\alpha < \beta$ (given $\beta < 0.5$), the delay is $T(1 - \beta)$, which in turn will restrain frequencies $n/[T(1 - \beta)]$ ($n = 1, 2, 3,...$) of the continuous spectrum, while in the same spectrum, peaks are distributed at frequencies higher than the harmonics of the nominal fundamental $1/T$. The position of the lightly touching finger determines the frequencies of dominance in the discrete spectrum. These will be found in the vicinity of $n/(T\alpha)$ ($n = 1, 2, 3,...$) and appear clustered.

For class two, where $\alpha > \beta$, the delay is $T\beta$, which restrains frequencies $n/(T\beta)$ ($n = 1, 2, 3,...$) of the continuous spectrum. However, due to an alone-standing impulse at the onset ($t = T\beta/2$), these frequencies will not be as much restricted as was the case for the restrained frequencies of class one. In the continuous spectrum, magnitude maxima will be found for frequencies $m/(T\alpha)$, ($m = 1, 2, 3,...$) and for $n/[T(1 - \alpha)]$, ($n = 1, 2, 3,...$), respectively. Where these two coincide, or nearly do so, the continuous spectrum will show major maxima, which again will have impact on the discrete spectrum if falling on harmonic frequencies. So, it is not quite as straightforward to predict the resulting outcome of bow and finger positions in class two. Some calculation is required.

It should be added that multiphonics is not restricted to open strings. On the double bass, "artificial" multiphonics can be produced chromatically from the lowest positions with the lightly touching finger up to three semitones higher than a firmly pressing thumb (i.e., $\alpha \geq \lambda^3 = 0.84$). It goes without saying that in higher positions, this interval can be increased, so that lower values of α are obtainable.

[1]Fernando Grillo composed the piece "Fluvine" per Contrabbasso in 1974. The piece introduces many novel techniques, including multiphonics.

[2]J.-P.e Robert: *Les Modes de jeu de la Contrabasse—Un Dictionnaire de son/Modes of Playing the Double Bass—A Dictionary of Sound* (Editions Musica Guild, Paris, 1995).

[3]M. Dresser, "A personal pedagogy,"*Arcana: Musicians on Music*, edited by J. Zorn (Granary Books, New York, 2000).

[4]M. Dresser, "Double bass multiphonics," The Strad **120** (1434), 72–75 (2009).

[5]M. Liebman, "Multiphonics Neue Moglichkeiten im Cellospiel (Multiphonics, New Possibilities in Cello Playing)," Das Orchester **4**, 14–19 (2001).

[6]Our simulation program FIDDLE is based on the concept developed by M. E. McIntyre and J. Woodhouse[7] and is described in the introduction of the dissertation by K. Guettler.[8,9]

[7]M. E. McIntyre and J. Woodhouse, "On the fundamentals of bowed-string dynamics," Acustica **43**, 93–108 (1979).

[8]K. Guettler, "The bowed string—On the creation of the Helmholtz motion, and on the development of anomalous low frequencies," Ph.D. dissertation, Royal Swedish Institute of Technology, Stockholm, Sweden, 2002.

[9]The introduction of K. Guettler's dissertation is available via the <http://kth.diva-portal.org/smash/get/diva2:9153/FULLTEXT01> (Last viewed 04/11/2011).

[10]In the simulations of Fig. 4, the double bass E-string Q values were programmed to lie between 60 and 200 for harmonics 1-25. To provide good stability, low-Q torsion with a characteristic wave resistance 2.5 times higher than the transverse ditto was included (although the magnetically recorded string-velocity signal used for input holds no information about torsion). For examples g and b, the absolute reflection coefficient, γ, at the finger position, α, was set to 0.5. See Sec. III A 1 for discussion on reflection coefficients.

[11]H. von Helmholtz, *On the Sensations of Tone* (Dover, New York, 1954), Appendix VI, pp. 384–387. Original publication: *Lehre von den Tonempfindungen* (Vieweg, Braunschweig, Germany, 1862).

[12]C. V. Raman, "On the mechanical theory of the vibrations of bowed strings and of musical instruments of the violin family, with experimental verifications of the results. I. Experiments with mechanically played violins," Proc. Indian Assoc. Cultivation Sci. **15** 1-158, 243–276 (1918).

[13]The Norbert Wiener deconvolution algorithm must be utilized as it, by adding a controlled amount of noise, prevents spectral zeroes to occur in the denominator.

[14]E. Schoonderwaldt, "The violinist's sound palette: Spectral centroid, pitch flattening and anomalous low frequencies," Acust. Acta Acust. **95**, 901–914 (2009).